Supporting Information

A Stable and Porous Iridium(III)-Porphyrin Metal-Organic Framework: Synthesis, Structure and Catalysis

Hao Cui,[a] Yingxia Wang,[a] Yanhu Wang,[a] Yanzhong Fan,[a] Li Zhang,*[a] and Cheng-Yong Su*[ab]

[a]MOE Laboratory of Bioinorganic and Synthetic Chemistry, Lehn Institute of Functional Materials, School of Chemistry and Chemical Engineering, Sun Yat-sen University, Guangzhou 510275, China

[b]State Key Laboratory of Organometallic Chemistry, Shanghai Institute of Organic Chemistry, Chinese Academy of Sciences, Shanghai 200032, China

Fax: (+86) 20-8411-5178

E-mail: zhli99@mail.sysu.edu.cn; cesscy@mail.sysu.edu.cn

Contents

1. General Methods S1

2. Physical Characterizations of Metalloporphyrin Ligands S2

3. Crystal Structure Data of Ir-PMOF-**1**(Zr) S3

4. Physical Characterizations of Ir-PMOF-**1**(Zr) S6

5. Comparison Study of Different Tetracarboxylated Porphyrin Based Zr-MOFs S9

6. Crystal Structure Data of Ir-PMOF-**2**(Zr) S11

7. Chemical and Thermal Stability Study of Ir-PMOF-**1**(Zr) S12

8. Dye Adsorption of Ir-PMOF-**1**(Zr) S15

9. Recycling Experiments S16

10. ICP Spectrometric Evaluation of Metal Leaching S17

11. Substrate Scope S18

1. General Methods.

The elemental analyses were performed with Perkin-Elmer 240 elemental analyzer. HRESI-MS was performed by using a Bruker Daltonics ESI-Q-TOF maXis4G. Infrared spectra on KBr pellets were collected with a Nicolet/Nexus-670 FT-IR spectrometer in the region of 4000-400 cm^{-1}. UV-vis spectra were tested on a Shimadzu/UV-3600 spectrophotometer. ^{1}H and ^{13}C NMR were recorded on Bruker AVANCE III 400MHz. PXRD patterns were recorded on SmartLab X-ray powder diffractometer (Rigaku Co.) at 40 kV and 30 mA with a Cu target tube. Thermogravimetric (TG) analyses were performed under an N_2 atmosphere at a heating rate of 10 °C min^{-1} by using a NETZSCH TG 209 system. X-ray photoelectron spectroscopy (XPS) was performed on a ULVAC PHI Quantera microprobe. Binding energies (BE) were calibrated by setting the measured BE of C 1s to 284.65 eV. ICP spectroscopy was conducted on a Spectro Ciros Vision ICP-OES spectrometer that is equipped with vacuum optics covering the spectral range from 175-777 nm, plasma power, 1300 w; coolant flow, 15.00 L/min; auxiliary flow, 0.80 L/min; nebulizer 0.70 L/min. The sorption isotherms for N_2 (77 K) and CO (77 K) gas were measured with an Autosorb-iQ2-MP gas sorption analyzer (Quantachrome, USA).

2. Physical Characterizations of Metalloporphyrin Ligands.

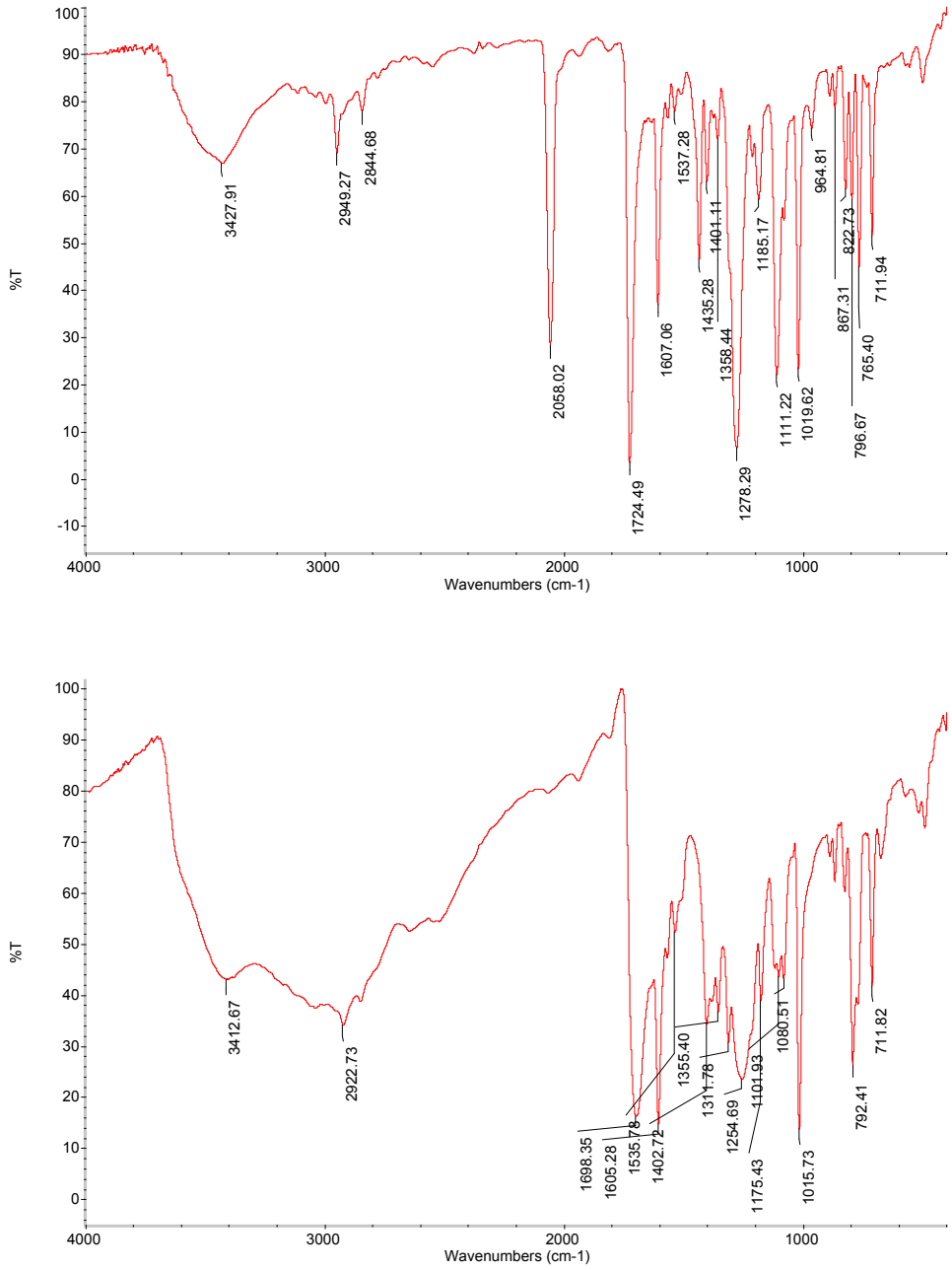

Figure S1. FT-IR spectra of Ir(TCPPCO$_2$Me)(CO)Cl (up) and Ir(TCPP)Cl (down).

3. Crystal Structure Data of Ir-PMOF-1(Zr).

Table S1. Crystal data and structure refinement parameters for Ir-PMOF-**1**(Zr).

MOF Code	Ir-PMOF-**1**(Zr)
Formula	$C_{144}H_{72}Cl_3Ir_3N_{12}O_{64}Zr_{12}$
Fw	4771.72
T/K	150(2)
Crystal system	cubic
Space group	*I*m-3m
a/Å	38.3937(2)
b/Å	38.3937(2)
c/Å	38.3937(2)
α/°	90
β/°	90
γ/°	90
Volume/Å^3	56595.2(9)
Z	4
ρ_{calc}g/cm^3	0.560
μ/mm^{-1}	3.421
F(000)	9176.0
Reflections collected	18180
Independent reflections	4293
Data/restraints/parameters	4393/155/103
R_{int}	0.0440
Goodness-of-fit on F^2	1.063
R1, *wR*2 [I>=2σ (I)]	0.0763, 0.2396
R1, *wR*2 [all data]	0.0919, 0.2559

Table S2. Selected bond lengths (Å) and bond Angles (º) for Ir-PMOF-**1**(Zr).

Bond Length (Å)		Bond Angle (º)	
Ir(1)-N(1)	2.037(5)	N(1)-Ir(1)-N(1)#1	90.002(5)
Ir(1)-N(1)#1	2.037(5)	N(1)-Ir(1)-N(1)#2	90.002(6)
Ir(1)-N(1)#2	2.037(5)	N(1)#1-Ir(1)-N(1)#2	179.4(6)
Ir(1)-N(1)#3	2.037(5)	N(1)-Ir(1)-N(1)#3	179.4(6)
Ir(1)-Cl(1)#2	2.308(19)	N(1)#1-Ir(1)-N(1)#3	90.002(5)
Ir(1)-Cl(1)	2.308(19)	N(1)#2-Ir(1)-N(1)#3	90.002(5)
Zr(1)-O(2)#4	2.085(3)	N(1)-Ir(1)-Cl(1)#2	90.3(3)
Zr(1)-O(2)#5	2.085(3)	N(1)#1-Ir(1)-Cl(1)#2	89.7(3)
Zr(1)-O(3)	2.154(4)	N(1)#2-Ir(1)-Cl(1)#2	89.7(3)
Zr(1)-O(1)	2.188(4)	N(1)#3-Ir(1)-Cl(1)#2	90.3(3)
Zr(1)-O(1)#6	2.188(4)	N(1)-Ir(1)-Cl(1)	89.7(3)
Zr(1)-O(4)#6	2.263(6)	N(1)#1-Ir(1)-Cl(1)	90.3(3)
Zr(1)-O(4)	2.263(6)	N(1)#2-Ir(1)-Cl(1)	90.3(3)
Zr(1)-O(2)	2.394(9)	N(1)#3-Ir(1)-Cl(1)	89.7(3)
Zr(1)-Zr(1)#7	3.4972(9)	Cl(1)#2-Ir(1)-Cl(1)	180
Zr(1)-Zr(1)#8	3.4972(9)	O(2)#4-Zr(1)-O(2)#5	115.9(4)
Zr(1)-Zr(1)#5	3.5097(15)	O(2)#4-Zr(1)-O(3)	68.32(18)
Zr(1)-Zr(1)#4	3.5097(14)	O(2)#5-Zr(1)-O(3)	68.32(18)
N(1)-C(7)#9	1.355(5)	O(2)#4-Zr(1)-O(1)	77.97(19)
N(1)-C(7)	1.355(5)	O(2)#5-Zr(1)-O(1)	146.1(2)
O(1)-C(1)	1.271(5)	O(3)-Zr(1)-O(1)	142.09(11)
O(2)-Zr(1)#4	2.085(3)	O(2)#4-Zr(1)-O(1)#6	146.1(2)
O(2)-Zr(1)#5	2.085(3)	O(2)#5-Zr(1)-O(1)#6	77.97(19)
O(3)-Zr(1)#7	2.154(3)	O(3)-Zr(1)-O(1)#6	142.09(11)
O(3)-Zr(1)#8	2.154(4)	O(1)-Zr(1)-O(1)#6	75.5(2)
		O(2)#4-Zr(1)-O(4)#6	136.7(3)
		O(2)#5-Zr(1)-O(4)#6	76.1(3)
		O(3)-Zr(1)-O(4)#6	80.3(2)
		O(1)-Zr(1)-O(4)#6	116.2(2)
		O(1)#6-Zr(1)-O(4)#6	75.12(19)
		O(2)#4-Zr(1)-O(4)	76.1(3)
		O(2)#5-Zr(1)-O(4)	136.7(3)
		O(3)-Zr(1)-O(4)	80.3(2)
		O(1)-Zr(1)-O(4)	75.12(19)
		O(1)#6-Zr(1)-O(4)	116.2(2)
		O(4)#6-Zr(1)-O(4)	69.6(4)
		O(2)#4-Zr(1)-O(2)	77.0(3)
		O(2)#5-Zr(1)-O(2)	77.0(3)
		O(3)-Zr(1)-O(2)	110.9(3)
		O(1)-Zr(1)-O(2)	76.44(18)
		O(1)#6-Zr(1)-O(2)	76.44(18)

	O(4)#6-Zr(1)-O(2)	144.20(17)
	O(4)-Zr(1)-O(2)	144.21(17)

Symmetry transformations used to generate equivalent atoms:#1 -y+3/2,-x+3/2,-z+1/2 #2 y-1/2,x+1/2,-z+1/2#3 -x+1,-y+2,z #4 -y+3/2,z+1/2,x-1/2 #5 z+1/2,-x+3/2,y-1/2 #6 -z+1,y,-x+1 #7 -z+1,x,-y+1 #8 y,-z+1,-x+1 #9 -x+1,y,z

4. Physical Characterizations of Ir-PMOF-1(Zr).

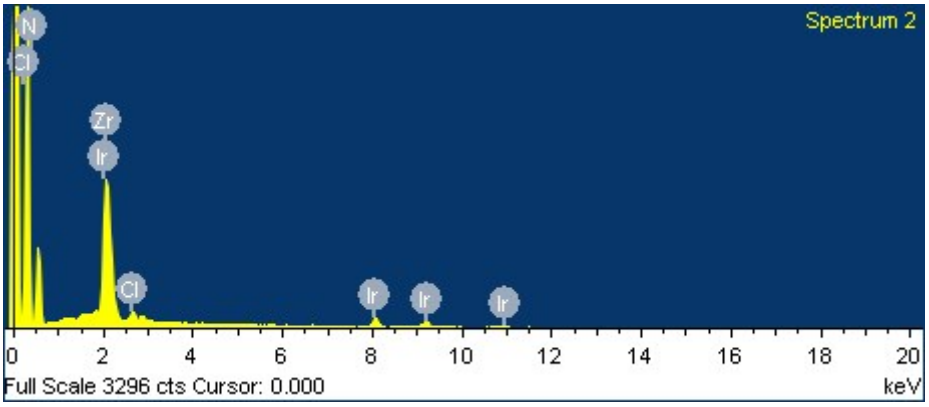

Figure S2. EDS spectrum of Ir-PMOF-**1**(Zr).

Table S3. Elemental analysis of Ir-PMOF-**1**(Zr) based on EDS experiment.

Element	Weight %	Atomic %
Zr	62.41	66.26
Ir	30.95	15.59
Cl	6.64	18.15

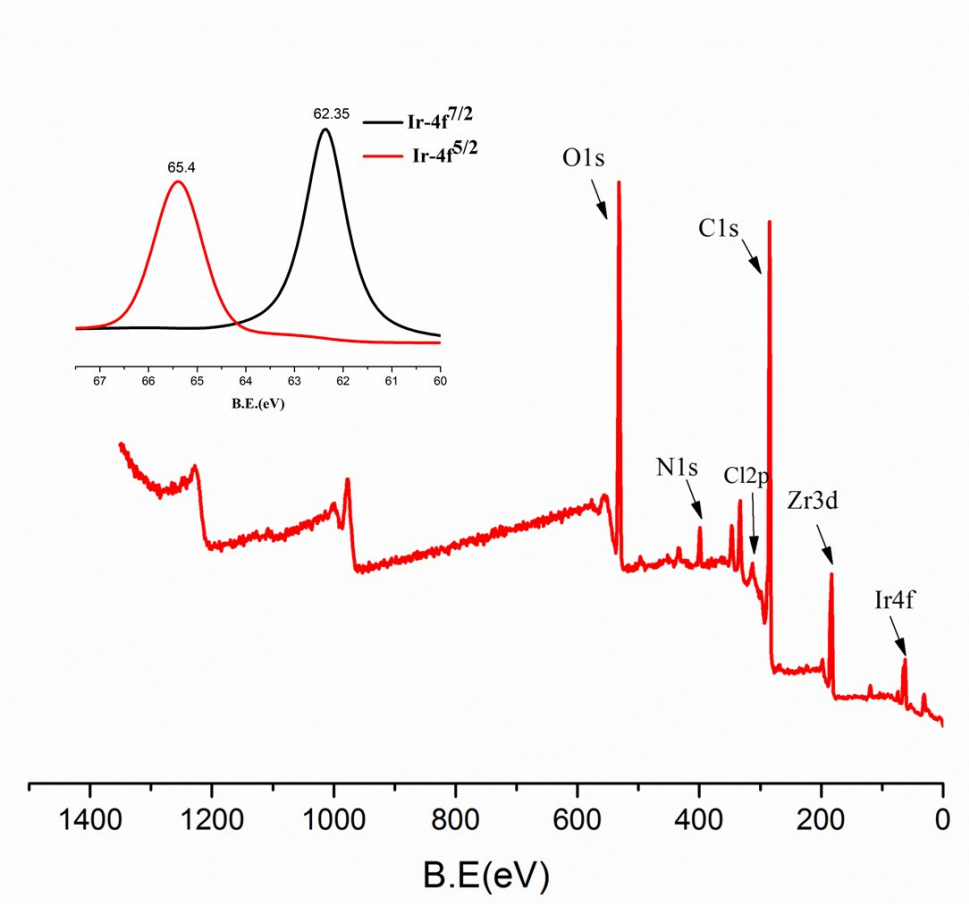

Figure S3. XPS spectrum of Ir-PMOF-**1**(Zr). The insert shows the peaks related to the Ir(III) atoms.

Table S4. Elemental analysis of Ir-PMOF-**1**(Zr) based on XPS experiment.

Element	Peak	Bond Energy (eV)	Atomic %
Zr	Zr 3d	182.76	2.66
Ir	Ir 4f	62.36	0.74
Cl	Cl 2p	197.85	0.79

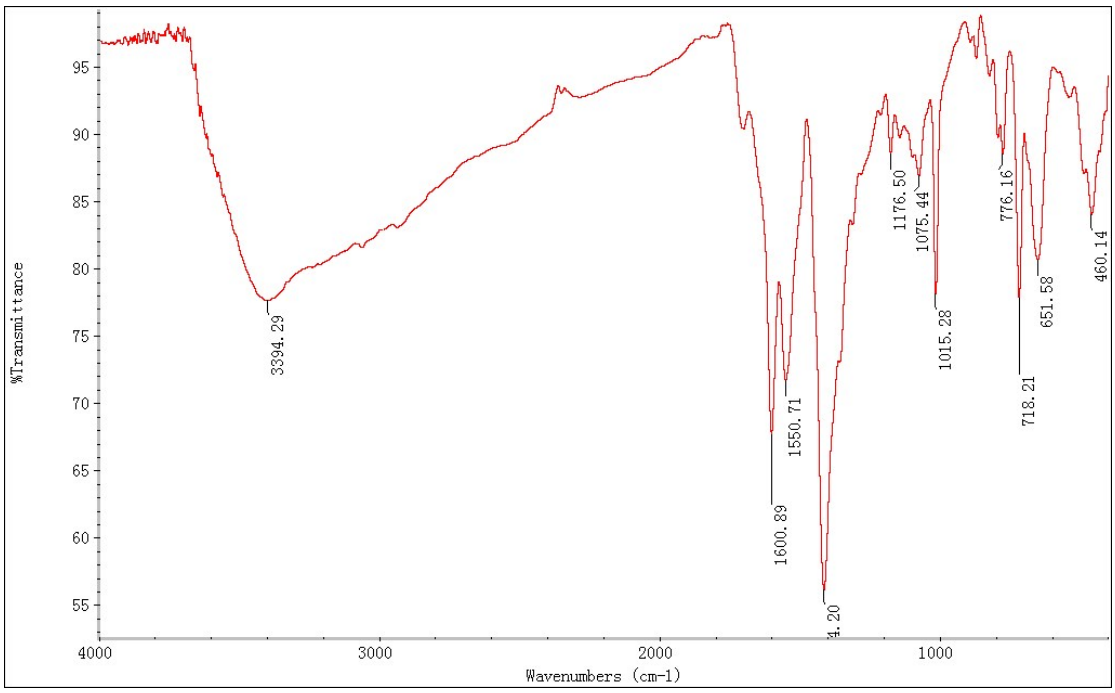

Figure S4. FT-IR spectrum of Ir-PMOF-**1**(Zr).

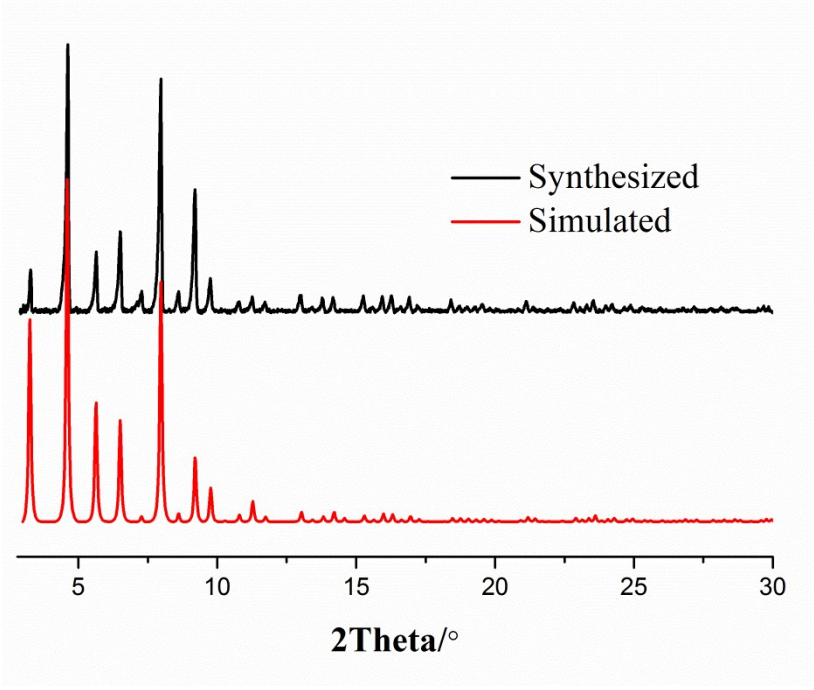

Figure S5. The experimental and simulated PXRD patterns of Ir-PMOF-**1**(Zr).

.

5. Comparison Study of Different Tetracarboxylated Porphyrin Based Zr-MOFs.

Table S5. Synthesis conditions and topology analysis of different tetracarboxylated porphyrin based Zr-MOFs.

MOF code	Ligand	Zr-cluster	T/℃（t/h）	Solvent	c (mmol/ml)	Zr/ligand ratio	Competing reagent	Topology
PCN-224(Ni)[1]	TCPP	$Zr_6(\mu_3\text{-}O)_8$	120ºC	DMF	$c_{M:}$ 0.021	3.6/1	benzoic acid	she
	4-connected	6-connected	24h		c_L: 0.0058		1mmol/mL	
PCN-222(Fe)[2]	TCPP(Fe)	$Zr_6(\mu_3\text{-}O)_8$	120ºC	DEF	$c_{M:}$ 0.037	5.2/1	benzoic acid	Kagome-like
	4-connected	8-connected	48h		c_L: 0.007		2.7mmol/mL	
MOF-545(Fe)[3]	TCPP(Fe)	$Zr_6(\mu_3\text{-}O)_8$	130ºC	DMF	$c_{M:}$ 0.011	2.9/1	formic acid	csq
	4-connected	8-connected	72h		c_L: 0.0037		0.5ml/mL	
CPM-99	TCBPP (H_2,Zn,Co,Fe)	$Zr_6(\mu_3\text{-}O)_8$	120ºC	DEF	$c_{M:}$ 0.023	3.3/1	benzoic acid	ftw
(H,Zn,Co,Fe)[4]	4-connected	12-connected	120h		c_L: 0.0068		0.3mmol/mL	
FJI-H6 (H_2,Cu)[5]	TCBPP(H_2,Cu)	$Zr_6(\mu_3\text{-}O)_8$	120ºC	DMF	$c_{M:}$ 0.032	5.9/1	benzoic acid	ftw
	4-connected	12-connected	96h		c_L: 0.0022		1mmol/mL	
PCN-228′[6]	TCBPP(Ni)	$Zr_6(\mu_3\text{-}O)_8$	120ºC	DMF	$c_{M:}$ 0.032	4.9/1	acetic acid	ftw-a
		12-connected	12h		c_L: 0.0065		0.2ml/mL	
PCN-221(Cu)[7]	TCPP(Cu)	$Zr_8(\mu_4\text{-}O)_6$	120ºC	DMF	$c_{M:}$ 0.015	2.6/1	benzoic acid	ftw
	4-connected	12-connected	12h		c_L: 0.0058		1mmol/mL	
Ir-PMOF-**1**(Zr)	TCPP	$Zr_6(\mu_3\text{-}O)_8$	120℃	DMF	c_M：0.04	7.2/1	benzoic acid	she
	4-connected	6-connected	48h		c_L：0.0055		2.3mmol/mL	
Ir-POMF-**2**(Zr)	TCPP	$Zr_8(\mu_4\text{-}O)_6$	150℃	DEF	c_M：0.04	4.4/1	benzoic acid	ftw
	4-connected	12-connected	12h		c_L：0.009		4.9mmol/mL	

References:

[1] PCN-224: D. Feng, W.-C. Chung, Z. Wei, Z.-Y. Gu, H.-L. Jiang, Y.-P. Chen, D. J. Darensbourg, H.-C. Zhou, *J. Am. Chem. Soc.*, 2013, **135**, 17105-17110.

[2] PCN-222: D. Feng, Z.-Y. Gu, J.-R. Li, H.-L. Jiang, Z. Wei, H.-C. Zhou, *Angew. Chem. Int. Ed.*, 2012, **51**, 10307-10310.

[3] MOF-545: W. Morris, B. Volosskiy, S. Demir, F. Gándan, P. L. McGrier, H. Furukawa, D. Cascio, J. F. Stoddart, O. M. Yaghi, *J. Am. Chem. Soc.*, 2015, **137**, 2199-2202.

[4] CPM-99: Q. Lin, X. Bu, A. Kong, C. Mao, X. Zhao, F. Bu, P. Feng, *J. Am. Chem. Soc.*, 2015, **137**, 2235-2238.

[5] FJI-H6: J. Zheng, M. Wu, F. Jiang, W. Su, M. Hong, *Chem. Sci.*, 2015, **6**, 3466-3470.

[6] PCN-228′: T.-F. Liu, D. Feng, Y.-P. Chen, L. Zou, M. Bosch, S. Yuan, Z. Wei, S. Fordham, K. Wang, H.-C. Zhou, *J. Am. Chem. Soc.*, 2015, **137**, 413-419.

[7] PCN-221: D. Feng, H.-L. Jiang, Y.-P. Chen, Z.-Y. Gu, Z. Wei, H.-C. Zhou, *Inorg. Chem.* 2013, 52, 12661-12667.

6. Crystal Structure Data of Ir-PMOF-2(Zr).

Due to the poor crystal data, the crystal structure of Ir-PMOF-**2**(Zr) couldn't be well refined. Single-crystal study shows that it crystallizes in space group *P*m-3m (a = 19.2487 (5) Å, b = 19.2487 (5) Å, c = 19.2487 (5) Å, α = 90º, β = 90º, γ = 90º), and is an isostructure of PCN-221.

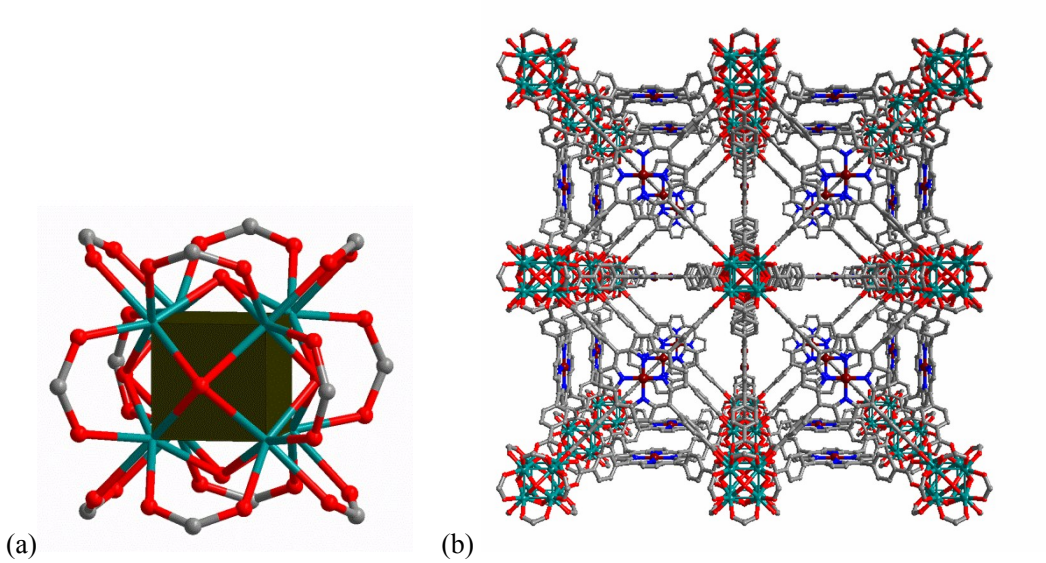

(a) (b)

Figure S6. Crystal structures of Ir-PMOF-**2**(Zr): (a) the 12-connected Zr_8 cluster; (b) the 3D framework nets (the axial Cl atoms are removed for clarity). Ir (dark red), Zr (teal), N (blue), O (red), Cl (bright green) and C (gray).

7. Chemical and Thermal Stability Study of Ir-PMOF-1(Zr).

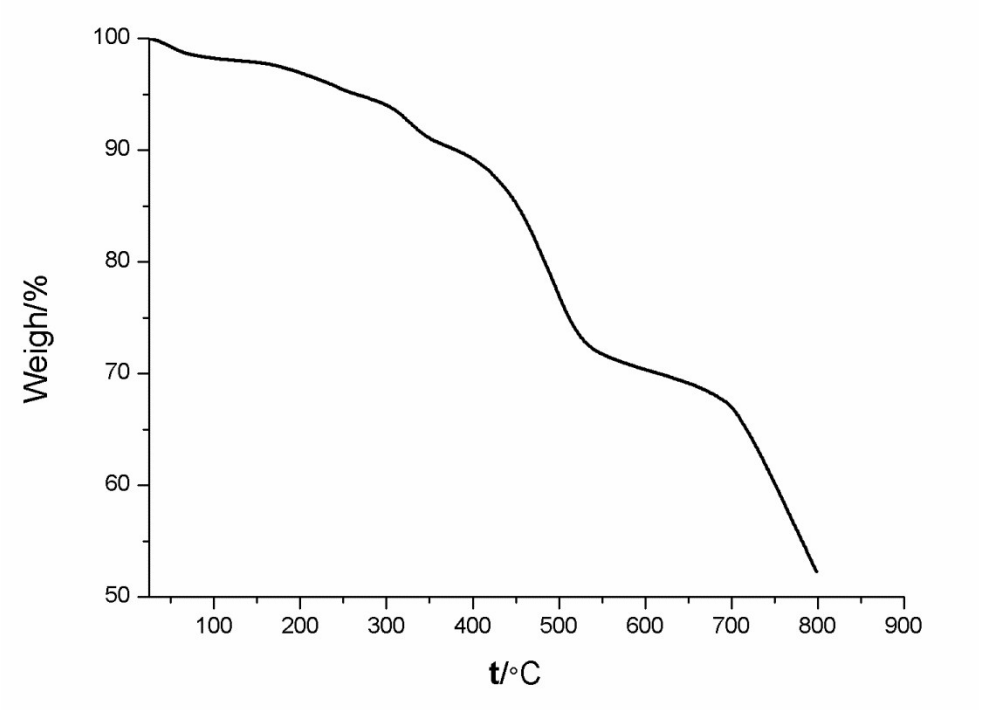

Figure S7. The TG curve of Ir-PMOF-**1**(Zr).

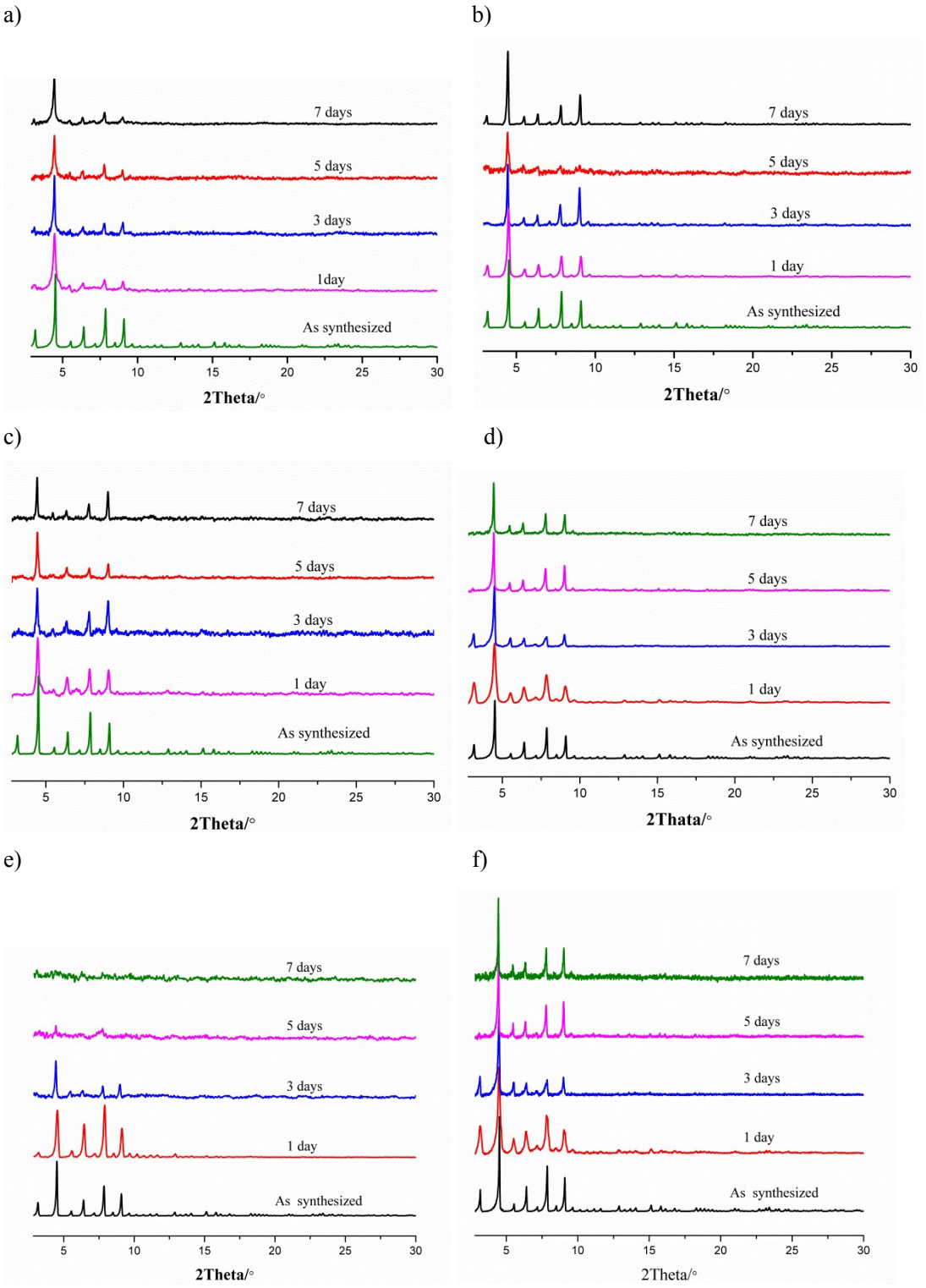

Figure S8. The chemical stability study of Ir-PMOF-**1**(Zr): The PXRD patterns upon treatments in different solvents for 1, 3, 5 and 7 days: a) ^{i}PrOH; b) acetonitrile; c) toluene; d) hexane; e) water; and f) DCM.

g) h)

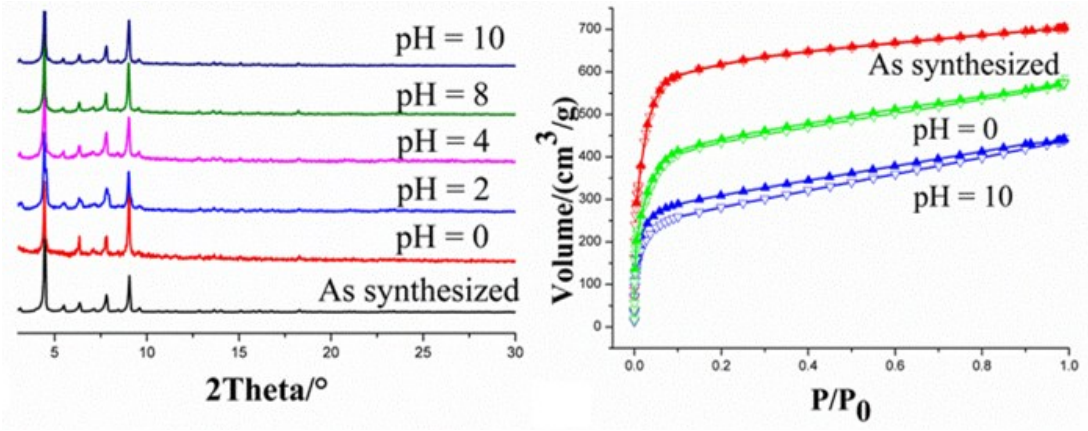

Figure S8. The chemical stability study of Ir-PMOF-**1**(Zr): The PXRD patterns upon treatments in different pH (0-10) aqueous solutions (g) and N_2 adsorption isotherms (h)

8. Dye Adsorption of Ir-PMOF-1(Zr).

The dye adsorption studies were carried out by immersing activated Ir-PMOF-**1**(Zr) (2 mg) in 8 mL of dye solution (20 mg L^{-1}). The dyes of orange gelb (OG) and methylene blue (MB) were dissolved in water. After adsorption, the dye concentration was determined by UV-vis spectroscopy. The wavenumbers for the UV-vis adsorption for OG and MB are 480 and 664 nm, respectively. After 24 h, around 9% of OG (corresponding to 14.4 μg) or 73% of MB (corresponding to 116.8 μg) was adsorbed in Ir-PMOF-**1**(Zr).

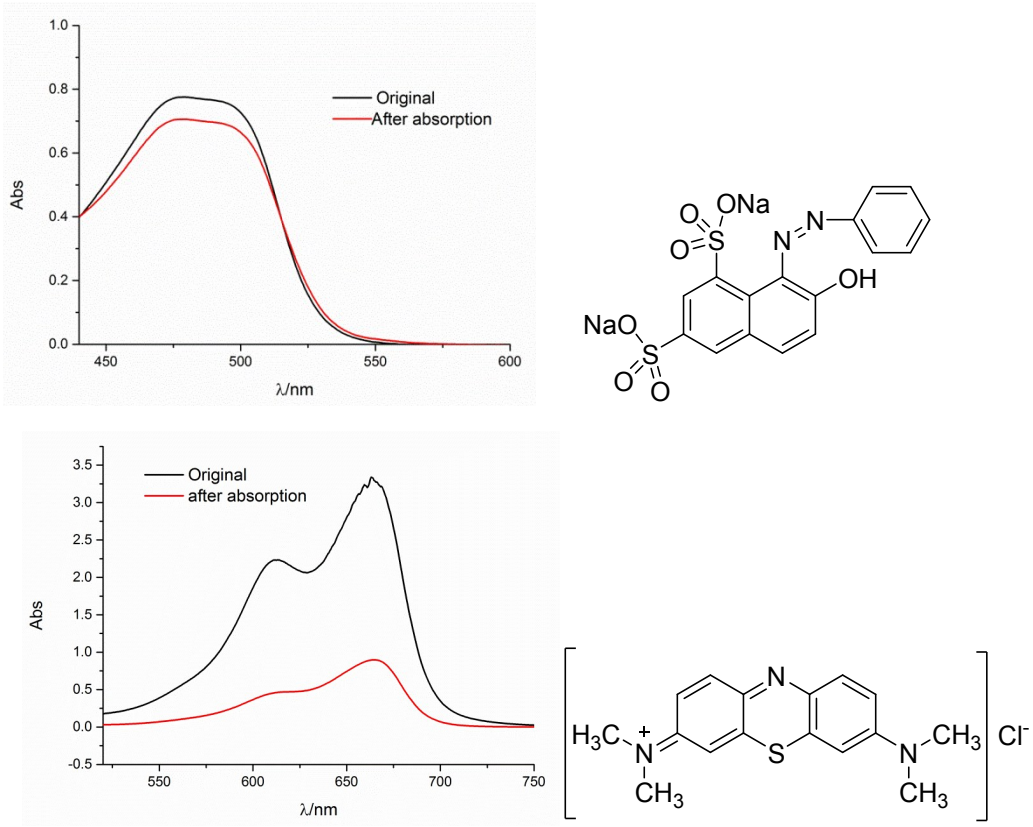

Figure S9. The UV-vis spectra for the dye uptake experiments of OG (up) and MB (down) for Ir-PMOF-**1**(Zr).

9. Recycling Experiments

Table S6. Recycling experiments of O-H insertion.

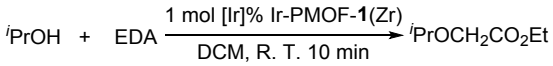

Run	Conversion (%)
1	94
2	92
3	94
4	88
5	86
6	90
7	91
8	88
9	88
10	64

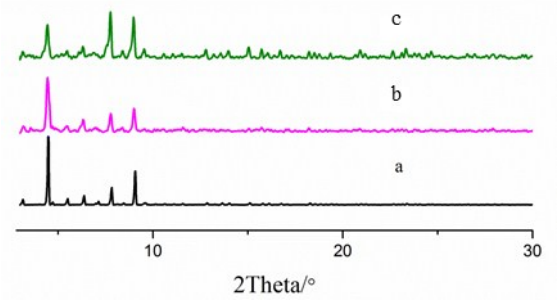

Figure S10. The PXRD patterns for Ir-PMOF-**1**(Zr) of as synthesized sample (a), after catalytic O-H insertion reactions (the first run (b) and the tenth run (c)).

10. ICP Spectrometric Evaluation of Metal Leaching

A solution of EDA (34.2 mg, 0.3 mmol, 1.0 eq) was added slowly to the solution of isopropanol (90 mg, 1.5 mmol, 5.0 eq) and Ir-PMOF-**1**(Zr) (4.7 mg, 0.003 mmol, 1 mol [Ir]%; containing 0.568 mg Ir) in DCM (1 mL). After the resulting solution was stirred at room temperature for 10 min, it was passed through a sand core funnel (G5) with a pad of celite, and washed with DCM. To examine the leached Ir content from the MOF catalyst Ir-PMOF-**1**(Zr) into the reaction solution, the combined filtrate was concentrated to dryness. Afterward, the dryness was treated with aqua regia (4 mL) and aqueous hydrogen dioxide (30 wt%, 1 mL). The whole mixture was allowed to stay at room temperature for 2 h and heated at 150 ˚C to reduce the total volume to about 0.5 mL (If possible, the digestion procedure might be repeated twice). The resulted colourless solution was diluted volumetrically with an aqueous solution of nitric acid (2%) to 25 mL, which was then evaluated by inductively coupled plasma optical emission spectrometer (ICP-OES) for Ir contents. The Ir contents were measured in ppm (mg L^{-1}) based on calibration curves obtained with a series of calibration standard solutions doped with different amount of Ir.

As for Ir-PMOF-**1**(Zr) catalyzed O-H insertion reaction, the measured Ir content was 0.014 ppm (0.00035 mg), and the leached Ir% should be 0.06%, using the calculation equation “100% × (0.00035 mg / 0.568 mg)”.

11. **Substrate Scope**

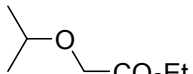

2a

^{1}H NMR (400 MHz, $CDCl_3$) of ethyl 2-isopropoxyacetate (**2a**): δ 4.18 (q, J = 7.2 Hz, 2H), 4.03 (s, 2H), 3.68 (m, 1H), 1.25 (t, J = 7.2 Hz , 3H), 1.22 (d, J = 6.1, 1.3 Hz, 6H)

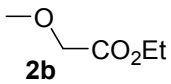

2b

^{1}H NMR (400 MHz, $CDCl_3$) of ethyl 2-methoxyacetate (**2b**): δ 4.25 (q, J = 7.1 Hz, 2H), 4.04 (s, 2H), 3.47 (s, 3H), 1.31 (t, J = 7.1 Hz, 3H).

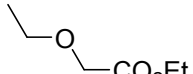

2c

^{1}H NMR (400 MHz, $CDCl_3$) of ethyl 2-ethoxyacetate (**2c**): δ 4.23 (q, J = 7.2 Hz, 2H), 4.08 (s, 2H), 3.61 (q, J = 7.2 Hz, 2H), 1.25 (t, J = 7.2 Hz, 3H), 1.21 (t, J = 7.2 Hz, 3H).

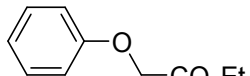

3a

^{1}H NMR (400 MHz, $CDCl_3$) of ethyl 2-phenoxyacetate (**3a**): δ 7.37 (t, J = 7.9 Hz, 1H), 7.09 (t, J = 7.4 Hz, 2H), 7.03 (d, J = 7.4 Hz, 2H), 4.71 (s, 2H), 4.39 – 4.32 (q, 2H), 1.37 (t, J = 7.2 Hz, 3H).

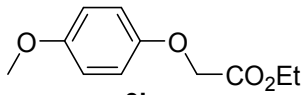

3b

^{1}H NMR (400 MHz, $CDCl_3$) of ethyl 2-(4-methoxyphenoxy)acetate (**3b**): δ 6.98-6.92 (m, 4H), 4.63 (s, 2H), 4.30 (q, J = 7.2 Hz, 2H), 3.78 (s, 3H), 1.33 (t, J = 7.2 Hz, 3H).

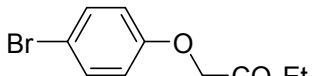

3c

^{1}H NMR (400 MHz, $CDCl_3$) of ethyl 2-(4-bromophenoxy)acetate (**3c**): δ 7.33 (d, J = 8.4 Hz, 2H), 6.76 (d, J = 8.4 Hz, 2H), 4.63 (s, 2H), 4.31 (q, J = 7.2 Hz, 2H), 1.34 (t, J = 7.2 Hz, 3H).